International Journal of Differential Equations and Applications
Volume **21**, No. 1 (2022), pages: 47-64
ISSN (Print): 1311-2872; ISSN (Online): 1314-6084;
url: https://www.ijdea.eu

ijdea.eu

TWO-SIDED BOUNDS OF EIGENVALUES USING CONFORMING AND NONCONFORMING FINITE ELEMENTS

A.B. Andreev[1], M.R. Racheva[2]

[1]Institute of Information and Communication Technologies
BAS, Sofia, BULGARIA
[2]Technical University of Gabrovo
Gabrovo, BULGARIA

ABSTRACT: The main goal of this paper is to present an original algorithm and numerical approach which gives two-sided bounds of eigenvalues for second-order elliptic operator. The method consists of finite element solving of the problem, making a choice of conforming elements and then constructing corresponding nonconforming interpolant of the approximate conforming eigenfunctions. Thus, solving only once the eigenvalue problem, we get upper and lower bounds for the exact eigenvalues. For this purpose we apply integral type finite elements, which use integral values on their edges or/and on the elements itselfs as degrees of freedom. From a practical point of view our aim is to use lowest possible order finite elements. Furthermore, the fact that the nonconforming interpolants use the nodal values of the conforming approximate eigenfunctions gives an obvious computational advantage.

Computational aspects of the algorithm are discussed. Finally, numerical experiments are also provided.

AMS Subject Classification: 65N30, 65N25
Key Words: conforming/nonconforming FEM, eigenvalue approximation, two-sided bound

Received: October 10, 2021 **Revised:** January 20, 2022
Published: March 1, 2022 **doi:** 10.12732/ijdea.v21i1.4
Academic Publications, Ltd. https://acadpubl.eu

1. INTRODUCTION AND PRELIMINARIES

It is well-known that for second-order self-adjoint elliptic operator the eigenvalues computed using standard conforming finite element method (FEM) are always above the exact ones. This fact comes from minimum-maximum characterization of the eigenvalues (see [5]). Therefore, it is an important and interesting problem to find methods giving lower bounds of the eigenvalues. So, our contribution here is to obtain two-sided bounds of eigenvalues using appropriate finite element spaces.

To express our idea more clearly, consider the following weak form eigenvalue model problem (EVP): Find a number $\lambda \in \mathbf{R}$ and a function $u \in V \equiv H_0^1(\Omega)$, $\|u\|_{0,\Omega} = 1$ such that

$$a(u,v) = \lambda(u,v), \tag{1}$$

where $a(u,v) = \displaystyle\int_\Omega \nabla u \cdot \nabla v \, dx\, dy \quad \forall u,v \in V.$

Here Ω is a bounded polygonal domain in $\mathbf{R}^2$ with boundary $\Gamma = \partial\Omega$. Given an integer $m \geq 0$, we denote by $H^m(\Omega)$ the usual $m-$th order Sobolev space on Ω with a norm $\|\cdot\|_{m,\Omega}$ and $(\cdot,\cdot)$ denotes the $L_2(\Omega)-$inner product.

The problem (1) has a countable sequence of real eigenvalues $0 < \lambda_1 \leq \lambda_2 \leq \ldots$ and the corresponding eigenfunctions $u_1, u_2, \ldots$ can be assumed to satisfy $\|u_j\|_{0,\Omega} = 1$; $(u_i, u_j) = \delta_{ij}, i, j \geq 1$.

The functions u_j belomg to the Besov space $B_2^{1+r,\infty}$ and in particular to the Sobolev space $H^{1+r-\varepsilon}(\Omega)$ for a small parameter $\varepsilon > 0$, where $r = 1$ if Ω is convex and $r = \pi/\omega$ otherwise (with ω being the largest inner angle of Ω) (see [7]).

Let $V_h \subset V$ be a conforming finite element space. The type of V_h will be specified later on. Then, the corresponding approximation of (1) is: Find a number $\lambda_h \in \mathbf{R}$ and a function $u_h \in V_h$, $\|u_h\|_{0,\Omega} = 1$ such that

$$a(u_h, v_h) = \lambda_h(u_h, v_h), \quad \forall v_h \in V_h. \tag{2}$$

We suppose that τ_h are uniform partitions of Ω generated from rectangles or rectangular triangles. Then h is the diameter of any element $K \in \tau_h$.

Let us introduce nonconforming finite element space $\widetilde{V}_h$ related to the partitions τ_h. For this purpose we define mesh-dependent bilinear form

$$a_h(u,v) = \sum_{K \in \tau_h} a_K(u,v), \quad u, v \in V,$$

where $a_K(u,v) = \int_K \nabla u \cdot \nabla v \, dx \, dy$.

Obviously, in case of conforming FEM, $a(\cdot,\cdot)$ and $a_h(\cdot,\cdot)$ coincide.

Here, we use integral type finite elements to obtain asymptotically lower bounds for eigenvalues. There are some results in this direction (see e.g. [2, 8] and references therein). But most of them use nonconforming finite element solutions. Obviously, it is valuable to find an interval as small as possible where the exact eigenvalue belongs to. But, it would be undesirable expensive to compute twice the eigenvalues – once using conforming FEM and second time by means of an appropriate nonconforming FEM.

Here, we propose a new procedure for determining bilateral estimates of λ. Namely, it is just sufficient to interpolate appropriately the already obtained conforming finite element eigenfunction.

2. BASIC RESULTS

First, we present some couples of elements (conforming and nonconforming) which could be applicable for our main algorithm implementation. Triangular and rectangular finite elements will be considered separately.

2.1. TRIANGULAR MESHES

2.1.1 Six-point conforming finite element (degrees of freedom are the values at the vertices and the integral values on the edges of the triangle) and Crouzeix-Raviart (C-R) nonconforming element (degrees of freedom are the integral values at the edges of the triangle) (Fig. 1).

2.1.2 Seven-point conforming triangle (degrees of freedom are the values at the vertices, the integral values on the edges of the triangle and the integral value over the triangle) and extended Crouzeix-Raviart (EC-R) nonconforming element (degrees of freedom are the integral values at the edges of the triangle and the integral value over the triangle) (Fig. 2).

Our basic result will be proved for the more complicated case 2.1.2. The 7-point 2-simplex finite element of reference $(K, \mathcal{P}, \Sigma)$ is defined as [3]:

- $K = \{(x,y): \ x \geq 0, \ y \geq 0, \ x+y \leq 1\}$ is the unit 2-simplex;
- $\mathcal{P}$ is a set of polynomials which satisfies $P_2 \subset \mathcal{P} \subset P_3$, where P_s is the space of all polynomials of degree, not exceeding s on K;

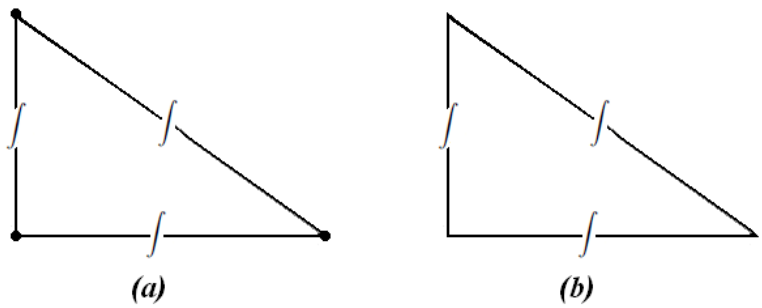

Figure 1: (a) 6-point conforming triangle; (b) Crouzeix-Raviart nonconforming triangular finite element

- $\Sigma = \left\{(x,y):\ x = \frac{i}{2};\ y = \frac{j}{2};\ i,j \in \{0,1,2\},\ i+j \leq 2 \cup \left(\frac{1}{3}, \frac{1}{3}\right)\right\}$ is a set of the Lagrangian interpolation nodes for the 6-node element adding the barycenter.

In the family of isoparametric triangular elements this is a unique finite element giving diagonalization of the mass matrix (lumped mass matrix) (see [3, 4]). This fact is due also to the presence of a suitable quadrature formula with positive coefficients exact for polynomials of P_3 (see [6], p. 184). On the other hand, a key role of some postprocessing methods play by certain locally supported, nonnegative functions (the seven-point basic functions in the case under consideration) that are commonly referred to as bubble functions [1].

Here, we propose an efficient method for obtaining eigenvalues estimates from below. For this purpose, we modify the 7-point conforming element by replacing the nodal values except for the values in the vertices with the integral values on the sides and in the element itself. So, an integral variant of 7-point triangular element is introduced.

The basic functions of the reference finite element are (Fig. 2(a)):

$$\varphi_1(x,y) = z^2 + 10xyz - 2(x+y)z, \qquad \varphi_4(x,y) = 6xy(1-5z),$$

$$\varphi_2(x,y) = 3x^2 + 10xyz - 2x, \qquad \varphi_5(x,y) = 6yz(1-5x),$$

$$\varphi_3(x,y) = 3y^2 + 10xyz - 2y, \qquad \varphi_6(x,y) = 6xz(1-5y),$$

$$\varphi_7(x,y) = 120xyz,$$

where $0 \leq x, y \leq 1,\ z = 1 - x - y$.

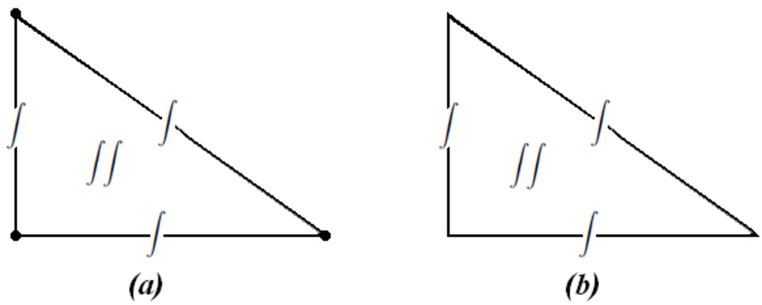

Figure 2: (a) 7-point conforming triangle; (b) Extended Crouzeix-Raviart non-conforming triangular finite element

For any test function v and $K \in \tau_h$, the degrees of freedom are $v(a_j)$, $\frac{1}{|l_j|}\int_{l_j} v(s)\,ds$ and $\frac{1}{|K|}\int\int_K v(x,y)\,dx\,dy$, where $a_j,\ j=1,2,3$ are the vertices, $l_j,\ j=1,2,3$ are the edges of K and $|l_j| = \int_{l_j} ds$; $|K| = \int\int_K dx\,dy$.

Thus, the corresponding approximation of (1) is the problem (2) by integral type 7-point finite elements.

Supposing that (2) is already solved, the point is to get a good approximation from below of λ in an easy and effective way.

Let us consider nonconforming finite element space of the extension of Crouzeix-Raviart element (EC-R). Its degrees of freedom could be obtained from those of the integral type 7-point 2-simplex element by removing the degrees of freedom in the element vertices (see Fig. 2(b)).

This nonconforming finite element space, denoted by $\widetilde{V}_h$ is defined as follows:

$$\widetilde{V}_h = \left\{v \in L_2(\Omega) : v_{|K} = span\{1, x, y, x^2+y^2\},\ v \text{ is integrally continuous on } \Omega\right\}.$$

On V we define the following interpolation operator: $\widetilde{i}_h : V \to \widetilde{V}_h$ in such a way that $\widetilde{i}_h v \in \widetilde{V}_h$ for any $v \in V$ and

$$\begin{aligned} &\int_{l_j} \widetilde{i}_h v\,ds = \int_{l_j} v\,ds,\ j=1,2,3; \\ &\int\int_K \widetilde{i}_h v\,dx\,dy = \int\int_K v\,dx\,dy, \end{aligned} \tag{3}$$

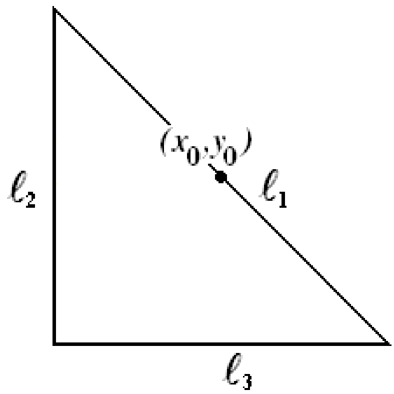

Figure 3: Triangular element

for $K \in \tau_h$ with edges $l_j, j = 1, 2, 3$.

Let us remind that the mesh-dependent bilinear form $a_h(\cdot,\cdot)$ approximates $a(\cdot,\cdot)$ on $\widetilde{V}_h + H_0^1(\Omega)$.

Lemma 1. *Let τ_h be uniform partition of Ω generated from rightangular triangular elements. Then for any $v \in V$ and $\widetilde{v}_h \in \widetilde{V}_h$*

$$a_h(\widetilde{i}_h v - v, \widetilde{v}_h) = 0. \tag{4}$$

Proof. If K_0 is a fixed reference triangle, results on arbitrary element $K \in \tau_h$ will be transfered from K_0 using an affine transformation.

The equations of the edges of K_0 are respectively:

$$l_1 : h_2(x - x_0) + h_1(y - y_0) = 0; \quad l_2 : x - x_0 = -\frac{h_1}{2}; \quad l_3 : y - y_0 = -\frac{h_2}{2},$$

where (x_0, y_0) is the midpoint of the hypotenuse and $h = \sqrt{h_1^2 + h_2^2}$ (Fig. 3).

The following notations for partial derivatives are adopted: $\partial_x \cdot = \dfrac{\partial \cdot}{\partial x}$, $\partial_y \cdot = \dfrac{\partial \cdot}{\partial y}$ and so on.

Thus, for any $v \in V$, $\widetilde{v}_h \in \widetilde{V}_h$

$$\begin{aligned} a_h(\widetilde{i}_h v - v, \widetilde{v}_h) &= \textstyle\sum_{K \in \tau_h} \int\int_K \nabla(\widetilde{i}_h v - v) \cdot \nabla \widetilde{v}_h \, dx\, dy \\ &= \textstyle\sum_{K \in \tau_h} \int\int_K \left(\partial_x(\widetilde{i}_h v - v) \partial_x \widetilde{v}_h + \partial_y(\widetilde{i}_h v - v) \partial_y \widetilde{v}_h \right) dx\, dy. \end{aligned} \tag{5}$$

Since $\widetilde{v}_h$ is an incomplete quadratic polynomial on K_0 and $\partial_{xy}\widetilde{v}_h = 0$, we obtain

$$\begin{aligned} \widetilde{v}_h(x, y) &= \widetilde{v}_h(x_0, y_0) + (x - x_0)\partial_x \widetilde{v}_h(x_0, y_0) + (y - y_0)\partial_y \widetilde{v}_h(x_0, y_0) \\ &+ \frac{1}{2}(x - x_0)^2 \partial_{xx} \widetilde{v}_h(x_0, y_0) + \frac{1}{2}(y - y_0)^2 \partial_{yy} \widetilde{v}_h(x_0, y_0). \end{aligned} \tag{6}$$

Then,

$$\partial_x \widetilde{v}_h(x,y) = \partial_x \widetilde{v}_h(x_0,y_0) + (x-x_0)\partial_{xx}\widetilde{v}_h,$$
$$\partial_y \widetilde{v}_h(x,y) = \partial_y \widetilde{v}_h(x_0,y_0) + (y-y_0)\partial_{yy}\widetilde{v}_h, \tag{7}$$

and in addition $\partial_{xx}\widetilde{v}_h = \partial_{yy}\widetilde{v}_h = const.$

Thus, we easily get:

$$\int\int_K \partial_x(\widetilde{i}_h v - v)\partial_x \widetilde{v}_h \, dx\, dy = \int\int_K \partial_x(\widetilde{i}_h v - v)\partial_x \widetilde{v}_h(x_0,y_0)\, dx\, dy$$

$$+\int\int_K \partial_x(\widetilde{i}_h v - v)(x-x_0)\partial_{xx}\widetilde{v}_h \, dx\, dy$$

$$= \partial_x \widetilde{v}_h(x_0,y_0)\left(\int_{l_1} - \int_{l_2}\right)(\widetilde{i}_h v - v)\, dy$$

$$+\partial_{xx}\widetilde{v}_h\left(\int_{l_1} - \int_{l_2}\right)(\widetilde{i}_h v - v)(x_0,y_0)\, dy - \int\int_K (\widetilde{i}_h v - v)\partial_{xx}\widetilde{v}_h \, dx\, dy.$$

Using the properties (3), the first and the third terms disappear and then

$$\int\int_K \partial_x(\widetilde{i}_h v - v)\partial_x \widetilde{v}_h \, dx\, dy = \partial_{xx}\widetilde{v}_h \int_{l_1} (x-x_0)(\widetilde{i}_h v - v)\, dy$$

$$+\frac{h_1}{2}\partial_{xx}\widetilde{v}_h \int_{l_2} (\widetilde{i}_h v - v)\, dy = \partial_{xx}\widetilde{v}_h \int_{l_1} (x-x_0)(\widetilde{i}_h v - v)\, dy.$$

Similarly, for the second term of (5) we obtain

$$\int\int_K \partial_y(\widetilde{i}_h v - v)\partial_y \widetilde{v}_h \, dx\, dy = \partial_{yy}\widetilde{v}_h \int_{l_1} (y-y_0)(\widetilde{i}_h v - v)\, dx.$$

Using that $\partial_{xx}\widetilde{v}_h = \partial_{yy}\widetilde{v}_h$, we prove the equality (4). □

2.2. RECTANGULAR MESHES

2.2.1 Eight-point serendipity conforming finite element (degrees of freedom are the values at the vertices and the integral values on the edges of the rectangle) and Rannacher-Tourek (rotated bilinear element; Q_1^{rot}) nonconforming element (degrees of freedom are the integral values at the edges of the rectangle) (Fig. 4).

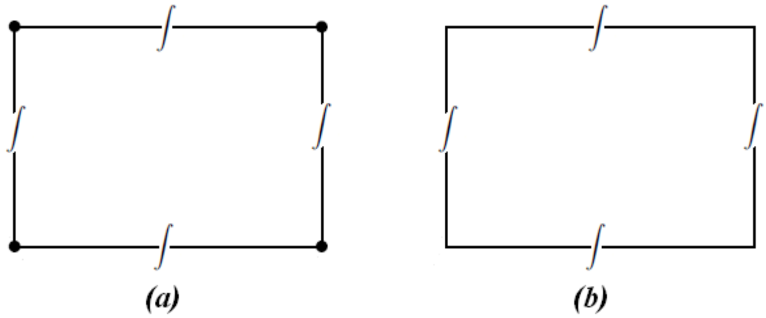

Figure 4: (a) 8-point serendipity conforming rectangle; (b) Rannacher-Tourek (Q_1^{rot}) nonconforming finite element

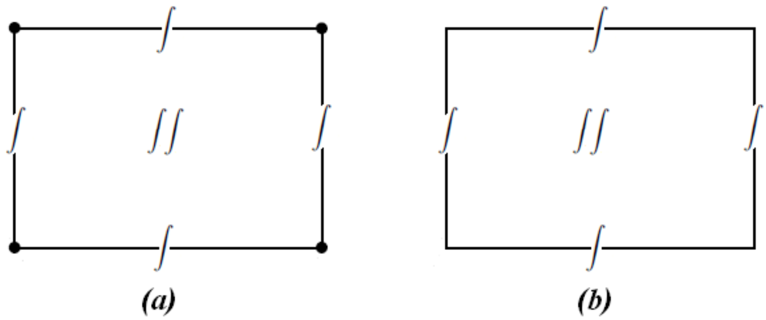

Figure 5: (a) 9-point conforming rectangle; (b) Extended Rannacher-Tourek (EQ_1^{rot}) nonconforming finite element

2.2.2 Nine-point conforming rectangular element (degrees of freedom are the values at the vertices, the integral values on the edges of the rectangle and the integral value over the rectangle) and extended Rannacher-Tourek (extended rotated bilinear element; EQ_1^{rot}) nonconforming element (degrees of freedom are the integral values at the edges of the rectangle and the integral value over the rectangle) (Fig. 5).

Lemma 2. *The results of the previous lemma are valid for considered rectangular cases.*

Proof. As in the previous case our considerations will be restricted for the more complicated elements 2.2.2 (see also Remark 1).

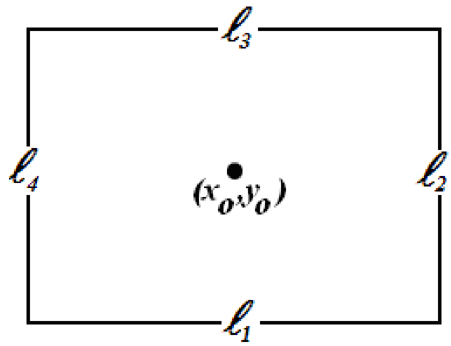

Figure 6: Rectangular element K_0

The basic functions of the reference finite element are (Fig. 2(a)):

$$\psi_1(x,y) = 3y^2 - 4y + 1, \qquad \psi_3(x,y) = 3y^2 - 2y,$$

$$\psi_2(x,y) = 3x^2 - 2x, \qquad \psi_4(x,y) = 3x^2 - 4x + 1,$$

$$\psi_5(x,y) = -6x^2 - 6y^2 + 6x + 6y - 1,$$

where $0 \le x \le 1,\ 0 \le y \le 1.$

In case of element 2.2.2 any function $\widetilde{v}_h$ is an incomplete quadratic polynomial on K_0 and $\partial_{xy}\widetilde{v}_h = 0$. Thus, the equalities (6) and (7) are fulfilled.

In addition: $\partial_{xx}\widetilde{v}_h = -\partial_{yy}\widetilde{v}_h = const.$

We calculate for $v \in V$ and $\widetilde{v}_h \in \widetilde{V}_h$

$$\int\int_{K_0} \partial_x(\widetilde{i}_h v - v)\partial_x\widetilde{v}_h\, dx\, dy = \partial_x\widetilde{v}_h(x_0,y_0)\left(\int_{l_2} - \int_{l_4}\right)(\widetilde{i}_h v - v)\, dy$$

$$+h\partial_{xx}\widetilde{v}_h\left(\int_{l_2} - \int_{l_4}\right)(\widetilde{i}_h v - v)\, dy - \int\int_{K_0}(\widetilde{i}_h v - v)\partial_{xx}\widetilde{v}_h\, dx\, dy \tag{8}$$

$$= -\int\int_{K_0}(\widetilde{i}_h v - v)\partial_{xx}\widetilde{v}_h\, dx\, dy.$$

Using the same arguments, it follows that

$$\int\int_{K_0} \partial_y(\widetilde{i}_h v - v)\partial_x\widetilde{v}_h\, dx\, dy = -\int\int_{K_0}(\widetilde{i}_h v - v)\partial_{yy}\widetilde{v}_h\, dx\, dy. \tag{9}$$

From (8) and (9) we have

$$\int\int_{K_0} \nabla(\widetilde{i}_h v - v) \cdot \nabla \widetilde{v}_h \, dx\, dy = \int\int_{K_0} (\widetilde{i}_h v - v)\ \Delta \widetilde{v}_h \, dx\, dy.$$

Havong in mind that $\Delta \widetilde{v}_h = const$, the last integral is equal to zero because of the condition

$$\int\int_{K_0} (\widetilde{i}_h v - v)\, dx\, dy = 0.$$

Summarizing over all $K \in \tau_h$, we get

$$a_h(\widetilde{i}_h v - v, \widetilde{v}_h) = 0.$$

□

Remark 1. *We use integral values of the test function v on the edges and over the element K instead of the values at the midpoints of l_j, $j = 1,2,3$ or $j = 1,2,3$ for rectangular and triangular element respevtively and at the centrer of K. These sets of degrees of freedom are affine equivalent. The reason of this approach will be discussed in the next section.*

Remark 2. *We presented the lowest order nonconforming planar elements verifying equality (4). On the other hand, we do not claim the uniqueness of such kind on nonconforming elements. Also, let us emphasize that (4) could be explored for some superconvergence finite element algorithms.*

Now, we introduce the following notation:

$$|v_h|^2_{a_h} = a_h(\widetilde{i}_h v_h, \widetilde{i}_h v_h), \quad \text{for any } v_h \in V + \widetilde{V}_h.$$

For our purposes, it is enough to assume the following interpolation inequality for $v \in V$:

$$|\widetilde{i}_h v - v|_{a_h} \geq C h^{2-\varepsilon}, \tag{10}$$

where ε is a small positive number.

Remark 3. *Let us note that this requirement is not much too restrictive. Indeed, interpolation for quadratic (conforming) finite elements by linear interpolant has an optimal order of approximation $\mathcal{O}(h)$ in $H^1(\Omega)-$norm.*

The following result is basic:

Theorem 1. *Let (λ_h, u_h) be an approximation of the exact eigenpair (λ, u) obtained from (2) using quadratic/biquadratic planar elements. If (10) is fulfilled, the number*

$$\widetilde{\Lambda}_h = a_h(\widetilde{i}_h u_h, \widetilde{i}_h u_h)$$

approximates λ from below when h is small enough, so that two-sided bounds of λ are obtained:

$$\widetilde{\Lambda}_h \leq \lambda \leq \lambda_h. \tag{11}$$

Proof. Taking into account that $u_h \in V_h$ and $\|u_h\|_{0,\Omega} = 1$, from equality (4) it follows:

$$\begin{aligned} a_h(\widetilde{i}_h u_h - u_h, \widetilde{i}_h u_h - u_h) &= a_h(\widetilde{i}_h u_h, \widetilde{i}_h u_h) - 2a_h(\widetilde{i}_h u_h, u_h) + a_h(u_h, u_h) \\ &= a(u_h, u_h) + a_h(\widetilde{i}_h u_h - u_h, \widetilde{i}_h u_h) - a_h(\widetilde{i}_h u_h, u_h) \\ &= a_h(u_h, u_h) - a_h(\widetilde{i}_h u_h, \widetilde{i}_h u_h) = \lambda_h - \widetilde{\Lambda}_h. \end{aligned}$$

Then

$$\lambda_h - \widetilde{\Lambda}_h = |\widetilde{i}_h u_h - u_h|^2_{a_h} \geq 0.$$

Since λ_h is a conforming approximation of λ by quadratic triangular or rectangular finite elements, we have (see [5]):

$$0 \leq \lambda_h - \lambda \leq C_1 h^4.$$

Furthermore, we obtain asymptotically for h sufficiently small the following inequality:

$$\begin{aligned} \lambda - \widetilde{\Lambda}_h = (\lambda - \lambda_h) + (\lambda_h - \widetilde{\Lambda}_h) &= -(\lambda_h - \lambda) + |\widetilde{i}_h u_h - u_h|^2_{a_h} \\ &\geq -C_1 h^4 + C_2 h^{4-2\varepsilon} \geq 0. \end{aligned}$$

Thus, (11) is proved. □

Based on the proved theorem, an algorithm can be fomulated:

Algorithm

1. Find eigenpairs (λ_h, u_h) from (2) by means of conforming quadratic/biquadratic finite element space V_h;
2. Construct $\widetilde{V}_h$ from V_h by eliminating the vertex degrees of freedom and then find the interpolation function $\widetilde{i}_h u_h \in \widetilde{V}_h$;
3. Calculate the number $\widetilde{\Lambda}_h = a_h(\widetilde{i}_h u_h, \widetilde{i}_h u_h)$ which approximates the exact eigenvalue λ asymptotically from below.

As a result of the proposed algorithm implementation, two-sided bounds (11) of eigenvalues λ are obtained.

3. COMPUTATIONAL ASPECTS

To implement the algorithm presented into the previous section, we use the couples of finite elements (conforming and nonconforming) proposed in 2.1 and 2.2:

- Six-point conforming finite element and Crouzeix-Raviart (C-R) nonconforming element;
- Seven-point conforming triangular finite element and extended Crouzeix-Raviart (EC-R) nonconforming element;
- Eight-point serendipity conforming finite element and Rannacher-Tourek (or rotated bilinear; Q_1^{rot}) nonconforming element;
- Nine-point conforming rectangular element and extended Rannacher-Tourek (or extended rotated bilinear; EQ_1^{rot}) nonconforming element.

Therefore, we solve the variational discrete problem (2) using conforming finite elements for V_h and as a result the approximate eigenvalues λ_h and the approximate eigenfunctions u_h are obtained. The approximate eigenvalues λ_h give upper bounds for the corresponding exact eigenvalues λ. Next, we interpolate the approximate eigenfunctions u_h by means of corresponding nonconforming finite element space. Obtaining the intepolants $\widetilde{i}_h u_h \in \widetilde{V}_h$ and calculating the numbers $\widetilde{\Lambda}_h = a_h(\widetilde{i}_h u_h, \widetilde{i}_h u_h)$, we get lower bounds for the exact eigenvalues λ.

Following the algorithm, we obtain two-sided bounds for the exact eigenvalues λ without solving the EVP twice (on conforming and nonconforming finite element space); we solve the EVP just once and thus we construct nonconforming intepolants of the conforming finite element eigenfunctions. This is just the main advantage of the proposed algorithm.

Due to the use of integral-type degrees of freedom for the conforming finite elements during the equation (2) numerical solving , an another advantage of the algorithm should be mentioned. In actual fact, solving (2) we get the approximate eigenfunction $u_h \in V_h$ into the form

$$u_h = \sum_{i=1}^{N} A_i \Phi_i(x, y),$$

where N is the number of the degrees of freedom for V_h, $\Phi_i(x, y), i = 1, 2, \ldots, N$ are the shape functions and $A_i, i = 1, 2, \ldots, N$ are either the values of u_h at the vertices of the elements from τ_h, or the integral values of u_h over the edges of the elements from τ_h and on the elements themselves.

On its part, the interpolant $\widetilde{i}_h u_h \in \widetilde{V}_h$ has a representation

$$\widetilde{i}_h u_h = \sum_{i=1}^{N_1} B_i \Psi_i(x,y),$$

where N_1 is the number of the degrees of freedom for $\widetilde{V}_h$, $\Psi_i(x,y), i = 1,2,\ldots,N_1$ are the shape functions and $B_i, i = 1,2,\ldots,N_1$ are the integral values of $\widetilde{i}_h u_h$ over the edges of the elements from τ_h and on these elements.

Due to use of integral type degrees of freedom for the conforming finite elements, once we have obtained u_h, and consequently $A_i, i = 1,2,\ldots,N$, the values $B_i, i = 1,2,\ldots,N_1$ are already known. They are among $A_i, i = 1,2,\ldots,N$ and to obtain them, we have just to elliminate these of A_i, which correspond to the vertices of the finite elements from the mesh. Thus, to calculate $a_h(\widetilde{i}_h u_h, \widetilde{i}_h u_h)$, we use the structure of the stiffeness matrix from (2), eliminating these columns and rows which correspond to the vertices of the finite element.

However, one may decide not to use integral type degrees of freedom for the conforming finite elements. Such being the case, the structure of the stiffeness matrix from (2) does not change and could be used again. But the coefficients $B_i, i = 1,2,\ldots,N_1$ should be calculated as linear combinations of $A_i, i = 1,2,\ldots,N$, which makes the computational procedure more complicated.

In any case, integral type degrees of freedom for the nonconforming finite elements have to be used (see Theorem 1).

The algorithm could be implemented using couples of finite elements (conforming and nonconforming), different from those considered in 2.1 and 2.2, e.g. nine-point conforming rectangular element and Q_1^{rot} nonconforming element, or seven-point conforming triangle and Crouzeix-Raviart (C-R) nonconforming element. All the same, a better strategy is to make the most of the resources which the corresponding conforming element gives.

4. NUMERICAL RESULTS

The results from numerical experiments given in this section serve as a verification and a confirmation of the validity, reliability and effectiveness of the proposed algorithm for obtaining two-sided bounds for eigenvalues.

Table 1: Approximations of the first three eigenvalues computed by 6-node triangular conforming FE ($\lambda_{j,h}$) and by C-R nonconforming interpolation ($\widetilde{\Lambda}_{j,h}$)

n		$j=1$	$j=2$	$j=3$
4	$\lambda_{j,h}$	2.006678062	5.054137112	5.104918114
	$\widetilde{\Lambda}_{j,h}$	1.881513965	4.418101457	4.288383144
8	$\lambda_{j,h}$	2.000449550	5.004048686	5.007461785
	$\widetilde{\Lambda}_{j,h}$	1.967022311	4.828857313	4.776079375
12	$\lambda_{j,h}$	2.000090174	5.000832398	5.001526627
	$\widetilde{\Lambda}_{j,h}$	1.985029796	4.921083851	4.895512927
16	$\lambda_{j,h}$	2.000028690	5.000269489	5.000494590
	$\widetilde{\Lambda}_{j,h}$	1.991516027	4.955005149	4.940188442
20	$\lambda_{j,h}$	2.000011782	5.000113244	5.000209144
	$\widetilde{\Lambda}_{j,h}$	1.994551051	4.971000836	4.961425791

For purpose of demonstration ot the method we proposed, we solve the problem (1) on square domain $\Omega = [0, \pi] \times [0, \pi]$.

The reason for this choice is that in this instance the exact eigenvalues are known. They are equal to $s_1^2 + s_2^2$, $s_{1;2} = 1, 2, \ldots$, so that $\lambda_1 = 2$, $\lambda_2 = \lambda_3 = 5$, $\lambda_4 = 8$, ...

For our numerical implementation we divide the domain Ω uniformly into $2n^2$ triangles or n^2 squares in case of triangular or rectangular elements, respectively. Thus the mesh parameter h is equal to $\dfrac{\pi\sqrt{2}}{n}$. The numerical experiment is implemented for $n = 4; 8; 12; 16; 20$.

The results from our numerical experiment for the first three eigenvalues are given in Table 1 – Table 4.

As expected, due to the use of conforming finite element method, the approximate values $\lambda_{j,h}$, $j = 1, 2, 3$ are greater than the exact eigenvalues λ_j, $j = 1, 2, 3$. The sequences $\{\lambda_{j,h}\}$, $j = 1, 2, 3$ obtained when the mesh parameter h decreases are decreasing for all of the conforming elements put into use. As regards the nonconforming interpolation implementation, as seen in Table 1 – Table 4, it results in an approxima-

Table 2: Approximations of the first three eigenvalues computed by 8-node rectangular conforming FE ($\lambda_{j,h}$) and by Q_1^{rot} nonconforming interpolation ($\widetilde{\Lambda}_{j,h}$)

n		$j=1$	$j=2$	$j=3$
4	$\lambda_{j,h}$	2.001091866	5.032026684	5.032037751
	$\widetilde{\Lambda}_{j,h}$	1.881513965	4.124185537	4.124191017
8	$\lambda_{j,h}$	2.000066432	5.002126594	5.004483905
	$\widetilde{\Lambda}_{j,h}$	1.949450862	4.748511061	4.750458945
12	$\lambda_{j,h}$	2.000013079	5.000451611	5.002891734
	$\widetilde{\Lambda}_{j,h}$	1.977322992	4.885339250	4.887582856
16	$\lambda_{j,h}$	2.000004134	5.000166314	5.002635721
	$\widetilde{\Lambda}_{j,h}$	1.987202566	4.934933146	4.937289058
20	$\lambda_{j,h}$	2.000001692	5.000088072	5.002571117
	$\widetilde{\Lambda}_{j,h}$	1.999994922	4.979244596	4.980117042

tion of the exact eigenvalues from below. When the mesh parameter h decreases, the sequences $\{\widetilde{\Lambda}_{j,h}\}$, $j = 1, 2, 3$ are increasing for all of the nonconforming interpolation implementations and go to the corresponding exact eigenvalue. Thereby the statement of Theorem 1 is confirmed.

Instead of applying the presented algorithm for obtaining two-sided bounds of the exact eigenvalues, one may obtain similar results solving numerically the problem (1) twice – by conforming finite elements and by corresponding nonconforming elements. The approximations $\widetilde{\lambda}_{j,h}$ obtained solving the EVP (1) on $\widetilde{V}_h$ have error of the same order as the approximate values $\{\widetilde{\Lambda}_{j,h}\}$, which are a result of the proposed algorithm implementation.

The number $\widetilde{\Lambda}_{j,h} = a_h(\widetilde{i}_h u_{j,h}, \widetilde{i}_h u_{j,h})$ could not be compared with $\widetilde{\lambda}_{j,h}$ which one may obtain solving the problem (1) by means of the corresponding nonconforming finite element. This assertion stands on the fact that $\widetilde{\Lambda}_{j,h}$ is not equal to Rayleigh quotient of any function from $\widetilde{V}_h$ and at that it is not known whether $\|\widetilde{i}_h u_{j,h}\|_{0,\Omega}$ is greater than

Table 3: Approximations of the first three eigenvalues computed by 9-node rectangular conforming FE ($\lambda_{j,h}$) and by EQ_1^{rot} nonconforming interpolation ($\widetilde{\Lambda}_{j,h}$)

n		$j=1$	$j=2$	$j=3$
4	$\lambda_{j,h}$	2.001024281	5.030616274	5.032574100
	$\widetilde{\Lambda}_{j,h}$	1.902219920	4.655142682	4.656420455
8	$\lambda_{j,h}$	2.000065532	5.002110541	5.004469411
	$\widetilde{\Lambda}_{j,h}$	1.974624003	4.901823878	4.903948840
12	$\lambda_{j,h}$	2.000013002	5.000450150	5.002890554
	$\widetilde{\Lambda}_{j,h}$	1.988641719	4.955268267	4.957598338
16	$\lambda_{j,h}$	2.000004120	5.000165987	5.002635517
	$\widetilde{\Lambda}_{j,h}$	1.993595054	4.974626877	4.977033035
20	$\lambda_{j,h}$	2.000001689	5.000087946	5.002571064
	$\widetilde{\Lambda}_{j,h}$	1.995896103	4.9837056000	4.986147765

1 or not.

For sake of comparison and illustration, in Table 4 we also give the values of $\widetilde{\lambda}_{j,h},\ j = 1,2,3$, computed by means of EC-R nonconforming elements. Let us observe, that for the numerical example under consideration the approximations $\widetilde{\Lambda}_{j,h}$ are even better than $\widetilde{\lambda}_{j,h}$.

Let us also note that, as it is seen from the numerical results, the proposed algorithm works not only for simple eigenvalues, but also in case of multiple eigenvalues.

In conclusion, the presented algorithm contributes to receiving two-sided bounds of the spectrum of second-order elliptic operators. It could be also applicable for more general second-order eigenvalue problems as well as for fourth-order eigenvalues problems. Its advantage is that the eigenvalue problem is solved only once and then with a simple interpolation procedure an approximation from below is obtained. Similarly, the construction of $\widetilde{V}_h$ is also easy to get (see Section 3). Thus the proposed method expands the use of nonconforming finite elements in a new aspect.

Table 4: Approximations of the first three eigenvalues computed by 7-node triangular conforming FE ($\lambda_{j,h}$), by EC-R nonconforming interpolation ($\widetilde{\Lambda}_{j,h}$) and by EC-R nonconforming FE ($\widetilde{\lambda}_{j,h}$)

n		$j=1$	$j=2$	$j=3$
	$\lambda_{j,h}$	2.005892076	5.036142495	5.087584349
4	$\widetilde{\Lambda}_{j,h}$	1.952135604	4.677483488	4.705826984
	$\widetilde{\lambda}_{j,h}$	1.903764937	4.236635509	4.258846597
	$\lambda_{j,h}$	2.000419980	5.003449620	5.007049395
8	$\widetilde{\Lambda}_{j,h}$	1.987315226	4.912752722	4.913833395
	$\widetilde{\lambda}_{j,h}$	1.974736916	4.789503228	4.791205288
	$\lambda_{j,h}$	2.000085596	5.000651616	5.001453225
12	$\widetilde{\Lambda}_{j,h}$	1.994314936	4.960446764	4.960650368
	$\widetilde{\lambda}_{j,h}$	1.988664673	4.904549262	4.904896264
	$\lambda_{j,h}$	2.000027409	5.000210644	5.000538034
16	$\widetilde{\Lambda}_{j,h}$	1. 996794489	4.977635149	4. 977760359
	$\widetilde{\lambda}_{j,h}$	1.993602390	4.945929497	4.946041332
	$\lambda_{j,h}$	2.000011259	5.000139752	5.000307228
20	$\widetilde{\Lambda}_{j,h}$	1.997562790	4.973734155	4.973734805
	$\widetilde{\lambda}_{j,h}$	1.995698360	4.965702041	4.965729041

REFERENCES

[1] M. Ainsworth, J.T. Oden, *A-posteriori Error Estimation in Finite Element Analysis*, Wiley, New York (2000).

[2] A. Andreev, M. Racheva, Two-sided bounds of eigenvalues of second- and fourth-order elliptic operators, *Appl. Math.*, **59** No. 4 (2014), 371-390.

[3] A. B. Andreev, T.D. Todorov, Lumped mass approximation for an isoparametric finite element eigenvalue problem, . *Sib. JNM* **2**(4) (1999), 295-308.

[4] A. B. Andreev, T.D. Todorov, Lumped mass error estimates for an isoparametric finite element eigenvalue problem. *Sib. JNM*, **3**(3) (2000), 215-228.

[5] I. Babuška, J. Osborn, Eigenvalue Problems, In: *Handbook of Numerical Analysis*, Vol. II, (Eds. P. G. Lions and Ciarlet P.G.), Finite Element Methods (Part 1), North-Holland, Amsterdam (1991), 641-787.

[6] P.G. Ciarlet, The Finite Element Method for Elliptic Problems. North-Holland, Amsterdam, New York, Oxford, 1978.

[7] P. Grisvard, Singularities in Boundary Priblems. MASSON and Springer-Verlag, 1985.

[8] Y.D. Yang, Z.M. Zhang, F.B. Lin, Eigenvalue approximation from below using non-conforming finite elements, SCIENCE CHINA, Mathematics (2010), Vol. 53 No. 1, 137-150.